Int. J. Electrochem. Sci., 12 **(2017)** 11677 – 11691, doi: 10.20964/2017.12.61

International Journal of
ELECTROCHEMICAL
SCIENCE
www.electrochemsci.org

Fractional Calculus in Electrical Impedance Spectroscopy: Poisson – Nernst – Planck model and Extensions

E. K. Lenzi[1,*], *H. V. Ribeiro*[2], *R. S. Zola*[2,3], *L. R. Evangelista*[2]

[1]Departamento de Fsica, Universidade Estadual de Ponta Grossa, Av. Carlos Cavalcanti, 84030-900 Ponta Grossa – PR, Brazil
[2] Departamento de Física, Universidade Estadual de Maringá, Avenida Colombo, 87020-900 Maringá – PR, Brazil
[3]Departamento de Física, Universidade Tecnológica Federal do Paraná, 86812-460 Apucarana – PR , Brazil
[*]E-mail: eklenzi@uepg.br

Received: 28 February 2017 / *Accepted:* 27 September 2017 / *Published:* 12 November 2017

We review some analytical results obtained in the context of the fractional calculus for the electrical spectroscopy impedance, a technique usually employed to interpret experimental data regarding the electrical response of an electrolytic cell. We start by reviewing the main points of the standard Poisson – Nernst – Planck model. After, we present an extension that incorporates fractional time derivatives of distributed order to the diffusion equation. Then, we include fractional time derivatives on the boundary conditions in order to face the problems that are characterized, in the low frequency limit, by a frequency dispersion and, consequently, leads to a response in the form $Z: 1/(i\omega)^{\gamma}$, where Z is the electrical impedance, $\omega = 2\pi f$, with f being the frequency of the applied voltage, and $0 < \gamma \leq 1$. This scenario is extended in order to encompass also the systems characterized by Ohmic electrodes. For these cases, by focusing the low frequency regime, we discuss the applicability of such extensions as a tool to describe experimental data. This analsis is applied in the description of the electrical impedance of electrolytic cells with Milli – Q water and a weak eletrolytic solution of KCl.

Keywords: fractional time derivative; boundary conditions; electrical response

1. INTRODUCTION

As straightforward as the concept of exponent is understood, i.e., $x^2 = xx$, the derivative $d^n f(x)/dx^n$ of a function $f(x)$ comes naturally in people's mind as the n^{th} application of the operator d/dx on the function $f(x)$. Historically, it is attributed to L'Hopital a query to Leibniz about n being

non-integer. Such conceptual change leads to a new branch of calculus, known as fractional calculus. Despite the enormous attention it draws in basic math, fractional calculus has found several applications over the years in many distinct fields. Such applications include numerical methods [1, 2, 3], signal processing [4], tensile and flexural strength in disordered materials [5], fractional fluid mechanics [6], fractional quantum mechanics [7, 8], fractional-order model of neurons [9] and many others. Among these, it has been recently applied in electrochemical systems, more specifically, for modeling electrical impedance spectroscopy.

The electrical spectroscopy impedance technique plays an important role from the experimental point of view to obtain information about the electrical properties of many different materials, in particular, those of liquids [10]. In general, the sample is submitted to an ac voltage of small amplitude to assure that its response to the external signal is linear. The impedance, $Z(\omega)$, is measured as a function of the frequency $f = \omega / 2\pi$ of the applied voltage, $V(t)$. An important point about this electrical measure, $Z(\omega)$, is the relation with physicochemical properties of the system such as diffusion coefficient, Debye's screening length, and number of particles. Thus, the models used to analyze these experimental data are the bridge between the electrical measure and the physicochemical which are related to the ionic properties of the system. Usually, the experimental results are essentially described in terms of the Poisson–Nernst–Planck (PNP) model [10, 11] or equivalent circuits [12, 13]. However, it is verified in several cases (see e.g. Ref. [14]), that these models are not able to describe the behavior of the experimental data in he whole range of frequencies and indeed some modifications are required. This aspect of the problem is more concerned with the low frequency interval in which the diffusion of ions and surface effects have both an important contribution to the electrical response.

One possibility to overcome this disagreement between the prediction of the models and experimental data is to incorporate fractional operators to the mathematical approach [15, 16, 17, 18]. Some pioneering works have investigated a number of diffusion models to address the electrochemical impedance by means of fractional calculus [19, 20, 21]. In these works, the impedance at high frequency was shown to behave as $Z \propto 1/(i\omega)^{\gamma/2}$, and, at low frequency, as $Z \propto 1/(i\omega)^{\gamma}$, where γ is the fractional coefficient. These results were a first generalization, using fractional calculus, proposed to account for the behavior of Warburg impedance [22, 23] (high frequency) and for the predictions of the constant–phase element (CPE) impedance model (low frequency). In these approaches, the effective electric field inside the sample is taken as the applied external field, i.e., no spatial distribution of charges is determined. This means that the influence of the ions on the spectroscopy impedance measurements is not taken into account in a complete manner. To achieve a more realistic description, a different strategy may be employed. It consists in solving the complete problem, i.e., to consider the presence of a drift term in the diffusion equation coupled with the Poisson equation. This problem was solved in the linear approximation by using fractional time derivatives in the bulk equation or in the boundary conditions [24, 25, 26, 27, 28, 30, 29]. In this scenario, the behavior at high frequency is given by $Z \propto 1/(i\omega)$ and $Z \propto 1/(i\omega)^{\gamma}$ at the low frequency.

Here, we review some analytic results obtained in Refs. [28, 29, 30, 31, 32] for the electrical impedance (or immittance). We start by reviewing the standard PNP model with blocking electrodes boundary conditions in Sec. 2; then, an extension of the PNP model that incorporates fractional time

derivatives of distributed order in the diffusion equation is presented in Sec. 3. Subsequently, we include fractional time derivatives in the boundary conditions in order to describe situations characterized, in the low frequency limit, by a dispersion on frequency, usually related to CPEs. For this extension, in Sec. 4, we analytically obtain the impedance and discuss its behavior in the low frequency limit. In the same section, we also present the results obtained for the impedance when the Ohmic term is added to the boundary conditions. In Sec. 5, we use the results presented in Sec. 4 to investigate the electrical response of electrical cells with Milli – Q water and a weak eletrolytic solution of KCl. In Sec. 6 and Sec. 7 are presented our discussions and conlusions.

2. IMPEDANCE AND PNP MODEL

Let us consider a cell in the shape of a slab of thickness d, limited by two flat surfaces placed in $z = \pm d/2$, where z is the axis, normal to the surfaces, of a Cartesian reference frame. This cell is initially filled with an isotropic liquid, inside which dimensionless ions (positive, with density $N_+(z,t)$ and negative, with density $N_-(z,t)$) are dispersed, forming a homogeneous medium of dielectric constant ε (for simplicity, hereafter measured in units of ε_0). The surfaces are supposed to be identical and the monovalent ions, of charge q, are supposed to have the same mobility $\mu_+ = \mu_- = \mu$; before the application of an external field, the liquid is locally and globally neutral. When the external field is turned on, the liquid becomes locally charged but remains globally neutral.

For the investigations connected with the impedance spectroscopy, we assume that the surfaces are prepared to work initially as blocking electrodes. In this case, for $V_0 = 0$, $N_+(z,t) = N_-(z,t) = N$, with N representing the equilibrium density of ions of positive and negative signs. If we neglect recombination of ions, we have $\int_{-d/2}^{d/2} N_+(z,t)dz = \int_{-d/2}^{d/2} N_-(z,t)dz = Nd,$ stating the *conservation of the number of particles*. If, on the other hand, $V_0 \neq 0$, $N_+(z,t) = N_-(-z,t)$. Since the amplitude of the external voltage is assumed to be small, the actual densities of ions only slightly differ from N and we can write $N_+(z,t) = N + n_+(z,t)$ and $N_-(z,t) = N + n_-(z,t),$ where $n_\pm(z,t)$ represents the bulk densities of ions due to the presence of the external field. Under these assumptions, the problem to obtain the current flowing through the cell can be solved by considering the three equations of the problem. The first two are the modified continuity equations

$$\frac{\partial}{\partial t} n_\pm(z,t) = -\frac{\partial}{\partial z} j_\pm(z,t), \tag{1}$$

in which the densities of currents for positive and negative ions are:

$$j_\pm(z,t) = -D\left[\frac{\partial}{\partial z} n_\pm(z,t) \pm \frac{Nq}{k_B T}\frac{\partial}{\partial z} V(z,t)\right], \tag{2}$$

where k_B is the Boltzmann constant, T is the absolute temperature, and D is the diffusion coefficient. The third one is Poisson's equation:

$$\frac{\partial^2}{\partial z^2}V(z,t) = -\frac{q}{\varepsilon}\left[n_+(z,t) - n_-(z,t)\right], \tag{3}$$

from which it is possible to obtain the electrical potential across the sample, $V(z,t)$. These are the fundamental equations of the Poisson – Nernst – Planck (PNP) model which may be solved by taking into account a specific boundary condition accounting for the surface effects.

Before obtaining the solutions for the previous equations, it is interesting to note that Eqs. (2) hold in the limit $|n_{\pm}(z,t)| = N$ if the amplitude of the external voltage is low. In this scenario, we are obtaining, from experimental point of view, the linear response of the system to an applied potential. These assumptions permits a linear approximation for these equations in order to analyze the electrical response of the system. A typical boundary condition to be considered is the *perfect blocking electrodes*, which in general is verified in several experimental scenarios if the region of low frequency is not considered. It is defined on $j_{\pm}(z,t)$ and can be written as

$$j_{\pm}\left(\pm\frac{d}{2},t\right) = 0, \tag{4}$$

and implies in an accumulation of charges in front of the electrodes' surfaces. Other effects on the surfaces such as adsorption – desorption processes or charge transfer require different boundary conditions. For the of potential $V(z,t)$ it is assumed that $V\left(\pm d/2,t\right) = \pm\left(V_0/2\right)e^{i\omega t}$.

This problem has been solved in detail by assuming that $V(z,t) = \phi(z)e^{i\omega t}$ is the form of the effective electric potential across the sample [11]. In this framework, the electrical impedance is defined as

$$Z(\omega) = V_0 e^{i\omega t} / I(t) = V_0 / \left(i\omega\varepsilon\phi'(d/2)S\right) \tag{5}$$

where $\phi'(z) = d\phi(z)/dz$ and S is the electrode area. From $Z(\omega)$ we obtain the real, $R = ReZ$, and the imaginary, $X = ImZ$, parts of the electrical impedance, which are the quantities experimentally detectable. By performing the calculations presented in Ref. [11], it is possible to show that

$$Z = -i\frac{2}{\omega\varepsilon S\beta^2}\left\{\frac{1}{\lambda_D^2\beta}\tanh\left(\frac{\beta d}{2}\right) + \frac{i\omega d}{2D}\right\}. \tag{6}$$

with

$$\beta = \frac{1}{\lambda_D}\sqrt{1 + i\frac{\omega}{D}\lambda_D^2}. \tag{7}$$

where $\lambda_D = \sqrt{\varepsilon k_B / (2Nq^2)}$ is the Debye's screening length. Thus, the electrical problem was formally solved and the impedance, defined in Eq. (5), was analytically obtained. In the low frequency limit, i.e., $\omega \to 0$, by writing $Z = R + iX$, it is possible to show that [11]

$$R \approx \frac{\lambda_D^2 d}{\varepsilon D S} \qquad \text{and} \qquad X \approx -2\frac{\lambda_D}{\varepsilon S \omega} \tag{8}$$

correspond to the main contributions for the electrical response. Note that the imaginary part of the impedance in this limit behaves as a capacitive element due to the particular form of the boundary condition. This behavior is different from the ones already reported (see e.g. Refs. [33, 34]) for experimental scenarios in which the low frequency limit is considered, and have stimulated modifications or extensions of this model like, for instance, by considering different groups of ions [35, 36] or other boundary conditions such as Chang – Jaffé [37] and Ohmic ones [38] among others. These extensions are anyway very useful and have been applied to several relevant physical situations, but the required low frequency behavior $Z:\ 1/(i\omega)^{\gamma}$ is always absent [29].

3. PNP MODEL – FRACTIONAL DIFFUSION EQUATIONS

In this section, we consider a formulation of the problem previously discussed in terms of fractional diffusion equations of distributed order. One of the motivations to consider the fractional diffusion equations is the possibility of incorporating effects which are not suitably described in terms of the usual approach. These effects are generally present in the low frequency limit where surface effects and diffusion have a pronounced role on the electrical response. A fractional time derivative of distributed order will be incorporated to the diffusion equation which appears from Eq. (1) and Eq. (2). A possible generalization is to consider

$$\frac{\partial}{\partial t} n_{\pm}(z,t) \to \int_0^1 d\gamma\, p(\gamma) \frac{\partial^{\gamma}}{\partial t^{\gamma}} n_{\pm}(z,t), \tag{9}$$

where $p(\gamma)$ is a distribution of γ with $\int_0^1 d\gamma\, p(\gamma) = 1$, in which

$$\frac{\partial^{\gamma}}{\partial t^{\gamma}} n_{\pm}(z,t) = \frac{1}{\Gamma(m-\gamma)} \int_{t_0}^{t} d\bar{t}\, \frac{n_{\pm}^{(m)}(z,\bar{t})}{\left(t-\bar{t}\right)^{\gamma+1-m}}, \tag{10}$$

$m-1 < \gamma < m$, $n_{\pm}^{(m)}(z,t)$ representing the $m-th$ derivative, and t_0 related to the conditions initially imposed to the system. For the present analysis, we consider $t_0 = -\infty$ to study the response of the system to the periodic applied potential defined above [39]. It is worth mentioning that the fractional diffusion equations of distributed order may present different regimes of diffusion [40, 41].

In the present case, the impedance is formally given by

$$Z = -i\frac{2}{\omega\varepsilon\beta^2 S}\left\{\frac{1}{\lambda_D^2\beta}\tanh\left(\frac{\beta d}{2}\right)+\frac{d}{2D}F(i\omega)\right\}, \tag{11}$$

where, now,

$$\beta = \frac{1}{\lambda_D}\sqrt{1+F(i\omega)\frac{\lambda_D^2}{D}}, \tag{12}$$

with

$$F(i\omega) = \int_0^1 d\gamma\, p(\gamma)(i\omega)^{\gamma}\,. \tag{13}$$

The presence of $F(i\omega)$ in Eqs. (11) and (12) is responsible for the incorporation of an arbitrary number of diffusive regimes to the description of ions through the sample. In addition, it is noteworthy that the general expression for the impedance, Eq. (11), has exactly the same functional form of Eqs. (6), if we consider $D_\gamma(i\omega) = i\omega D / F(i\omega),$ which can be faced now as its particular case. The presence of reaction terms can be incorporated to $F(i\omega)$ as done in Ref. [42]. The changes produced by the fractional time derivative of distributed order on the impedance response can be better understood by taking into account a particular case. For instance, consider $p(\gamma) = A\delta(\bar{\gamma}-1)+B\delta(\bar{\gamma}-\gamma)$ with $A+B=1$ which may be related to different regimes of diffusion as pointed out in Ref. [40, 41].

Results obtained from Eq. (11) are illustrated in Fig. 1 for different values of γ. We observe that in the low frequency limit the behavior is capacitive, as in the case treated in the previous section. The main changes produced by this new formalism are observed on the relaxation processes, due to the bulk effects related to the fractional time derivatives present in the diffusion equation. These features can also be verified by analyzing the asymptotic behavior of Eq. (11) for $\omega \to 0$. The contributions, for $\gamma > 1/2$ without loss of generality, for the real and imaginary parts of Eq. (11) are, respectively,

$$R \approx \frac{d\lambda_D^2}{DS\varepsilon}\left(A+\frac{B}{\omega^{1-\gamma}}\sin\left(\frac{\pi}{2}\gamma\right)\right) \tag{14}$$

and

$$X \approx -2\frac{\lambda_D}{S\varepsilon\omega}. \tag{15}$$

Thus, we verify that the real part of the impedance is directly influenced by the fractional time derivative of distributed order while the imaginary part presents the same behavior as before. These results suggest that changes on the boundary conditions are needed to obtain a different behavior for the imaginary part of the impedance.

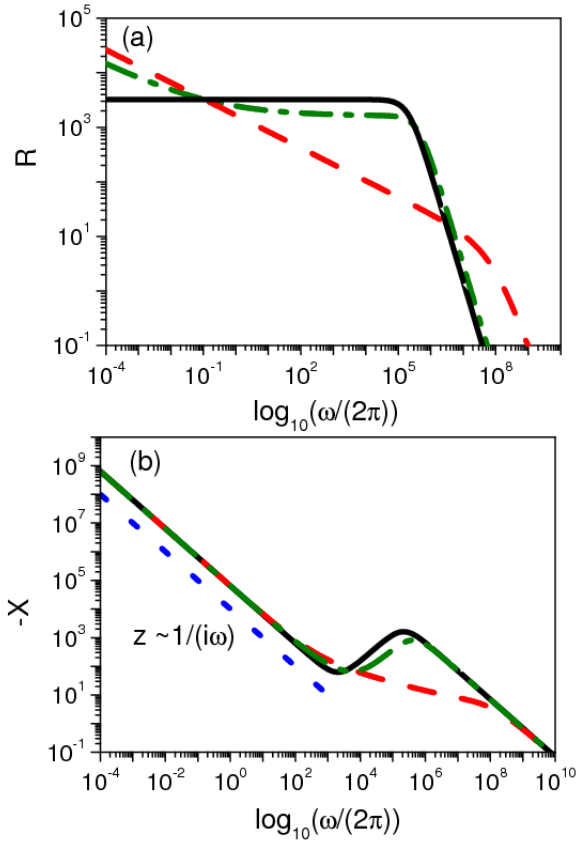

Figure 1. Behavior of the real and imaginary parts of the impedance, $R=Re\,Z$, and $X=Im\,Z$ versus the frequency are illustrated in Figs. 1a and 1b. The black (solid) line corresponds to the standard case, i.e., $p(\gamma)=\delta(\gamma-1)$, the red dashed line is a fractional case with $p(\gamma)=\delta(\gamma-\bar{\gamma})$ with $\bar{\gamma}=0.7$, and the green dashed–dotted line is a distributed case with $p(\gamma)=(1/2)\delta(\gamma-1)+(1/2)\delta(\gamma-\bar{\gamma})$. We considered, for simplicity, $S=3.14\times10^{-3}\,m^2$, $\varepsilon=82\varepsilon_0$, $D=2.85\times10^{-9}\,m^2/s$, $d=10^{-3}\,m$, and $\lambda=4.58\times10^{-8}\,m$. The blue dotted line was incorporated in Fig. 1b to evidence the asymptotic behavior in the low frequency limit.

4. PNP MODEL – SURFACE EFFECTS: BOUNDARY CONDITIONS

The results obtained by means of the extension of the PNP model to a fractional diffusion equation of distributed order evidence its potential application to those situations in which the bulk effects are relevant for the electrical response. To account for the effects related to the surfaces different boundary conditions are required. From the phenomenological point of view, a relevant guide to formulate a suitable boundary condition to successfully describe the experimental data is the behavior of the imaginary part of the impedance in the low frequency limit. Thus, the next essential ingredient to be added to this model is to extend the boundary conditions in such a way to encompass effects which are not taken into account in the usual treatment and are intrinsically connected with the boundary conditions. An approach of this kind was presented, for instance, in Refs. [31, 32], where the boundary condition were essentially assumed to be

$$j_{\pm}\left(\pm d/2,t\right) = \pm \int_0^1 d\bar{\eta}\int_{-\infty}^{t} dt'\kappa(t-t',\bar{\eta})\partial_t^{\bar{\eta}} n_{\pm}\left(\pm d/2,t'\right), \tag{16}$$

where the freedom in choosing $\kappa(t,\bar{\eta})$ permits the description of surface effects such as adsorption–desorption if we consider, for example, $\kappa(t,\bar{\eta}) = \left(\tilde{\kappa}/\tau\right)e^{-t/\tau}\delta(\bar{\eta}-1)$ which accounts for the kinetic process governed by a linearized Langmuir equation [11], or charge transfer, if we consider which $\kappa(t,\bar{\eta}) = \tilde{\kappa}\delta(t-t')\delta(\bar{\eta})$ [37]. In this way as well, Eq. (16) embodies different situations and may be surely useful to describe experimental scenarios characterized by anomalous diffusion, as discussed in Refs. [43, 44, 45]. The impedance obtained when considering the condition (16) is [29, 30]

$$Z = \frac{2}{i\omega\varepsilon S\beta^2}\frac{\tanh\left(\beta d/2\right)/\left(\lambda^2\beta\right) + d/\left(2D\right)\mathcal{E}}{1+\bar{\kappa}(i\omega)\left(1+i\omega\lambda^2/D\right)\tanh\left(\beta d/2\right)/\left(\beta i\omega\lambda^2\right)}, \tag{17}$$

where $\mathcal{E} = F\left(i\omega\right) + \beta\bar{\kappa}(i\omega)\tanh\left(\beta d/2\right)$ and $\bar{\kappa}(i\omega) = e^{-i\omega t}\int_0^1 d\bar{\eta}(i\omega)^{\bar{\eta}}\int_{-\infty}^{t}\kappa(t-t',\bar{\eta})e^{i\omega t'}\,dt'$. It is worth to mention that this result for Z can be related with the electrical impedance found in Refs. [26] and [27] if we perform the substitution $\bar{\kappa}(i\omega)/(i\omega) \to \bar{\kappa}(i\omega)$. Figure 2 shows the trend of Eq. (17) by taking into account two different dynamical scenarios for the surfaces. Particularly, the behavior of the imaginary part of the impedance in the low frequency limit is different from the ones exhibited in Fig. 1, which are purely capacitive, i.e., $Z:\ 1/(i\omega)$, when fractional operators are employed only in the bulk equation. By taking in Eq. (17) the limit of low frequency, i.e., $\omega \to 0$, this fact can be made more evident and indeed it is possible to show that

$$Z \approx \frac{2\lambda_D}{\varepsilon S}\frac{1}{i\omega + \bar{\kappa}(i\omega)/\lambda_D} + \frac{\lambda_D^2 d}{\varepsilon S D}. \tag{18}$$

In Eq. (18), the real part can be directly associated to bulk effects, in a way similar to the one found in the cases worked out in previous sections. It is noteworthy that the imaginary part exhibits instead a dependence on $\bar{\kappa}(i\omega)$, and consequently, thus explicitly showing how the surface influences the system in the low frequency limit. By a suitable choice of $\bar{\kappa}(i\omega)$, the impedance predicted by this model is able to reproduce many different behaviors, as illustrated in Fig. 2 for the cases obtained when we consider $\bar{\kappa}(i\omega) = \bar{\kappa}_1 + \bar{\kappa}_2(i\omega)^{\delta_2}$. This expression for $\bar{\kappa}(i\omega)$ is a superposition between two different effects, namely a charge transfer and a capacitive-like behavior for $\delta_2 \neq 1$, which may be associated to an accumulation and/or adsorption–desorption process at the electrode surfaces. In addition, Fig. 2 also shows that it is possible to explain the asymptotic behavior $Z:\ 1/(i\omega)^{\delta}$ (with $0 < \delta \leq 1$) found in several experimental scenarios [28, 26, 27, 34].

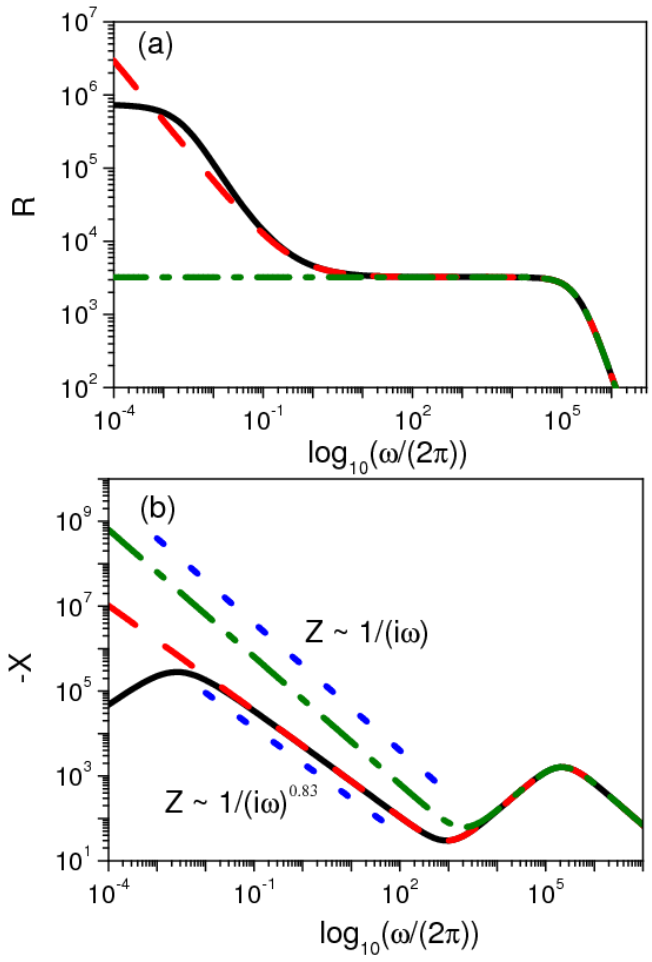

Figure 2. Behavior of the real and imaginary parts of the impedance, $R = Re\,Z$, and $X = Im\,Z$ versus the frequency are illustrated in Figs. 2a and 2b. The black (solid) line corresponds to the case $\bar{\kappa}(i\omega) = \bar{\kappa}_1 + \bar{\kappa}_2 (i\omega)^{\delta_2}$, the red dashed line is the case $\bar{\kappa}(i\omega) = \bar{\kappa}_2 (i\omega)^{\delta_2}$, and the green dashed–dotted line is the standard case $\bar{\kappa}(i\omega) = 0$. We considered, for simplicity, $S = 3.14 \times 10^{-3}\ m^2$, $\varepsilon = 82\varepsilon_0$, $D = 2.85 \times 10^{-9}\ m^2 / s$, $d = 10^{-3}\ m$, $\bar{\kappa}_1 = 9.5 \times 10^{-8} \mathrm{m/s}$, $\delta_2 = 0.83$, and $\bar{\kappa}_2 = 1.47 \times 10^{-5} \mathrm{m/s^{1-\delta_2}}$, and $\lambda = 4.58 \times 10^{-8}\ m$. The blue dotted lines were incorporated in Fig. 2 to evidence the behavior of the impedance in the intermediate and low frequency range.

To complete our discussion about the electrical response and the extensions of the PNP model, it is possible to add to Eq. (16) the Ohmic contribution of the electrodes. In this case, it may be rewritten as

$$j_{\pm}(\pm d/2, t) = \pm\, k_{\pm,e} E\left(\pm d/2, t\right) \pm \int_0^1 d\bar{\eta} \int_{-\infty}^{t} dt' \kappa(t - t', \bar{\eta}) \partial_{t'}^{\bar{\eta}} n_{\pm}\left(\pm d/2, t'\right) \tag{19}$$

In Eq. (19), $E\left(z,t\right)$ is the electric field across the sample and $k_{\alpha,e}$ represent the parameters of the Ohmic model measured, e.g. in $1/(Vms)$ in the SI system. Thus, the first term simply states that the

ionic current density on the electrode is proportional to the surface electric field whereas the second term is the boundary condition stated before. For this case it is also possible to find the following analytical expression for the impedance [31]:

$$Z = \frac{2}{S\varepsilon\beta\Delta(i\omega)}\left\{\frac{1}{\lambda_D^2\beta}\tanh\left(\beta\frac{d}{2}\right)+\frac{d}{2D}E(i\omega)\right\}, \tag{20}$$

with

$$\Delta(i\omega) = \frac{1}{\beta}\left\{\frac{1}{\lambda_D^2}+\frac{\chi}{D}\left[F(i\omega)+\omega_e\right]\right\}\left(i\omega+\omega_e\right)+\left\{\frac{1}{\lambda_D^2}+\frac{\chi}{D}\left[i\omega+\omega_e\right]\right\}\bar{\kappa}(i\omega)\tanh\left(\beta\frac{d}{2}\right), \tag{21}$$

where $\bar{E}(i\omega) = \chi\left[F(i\omega)+\omega_e\right]+\chi\beta\bar{\kappa}(i\omega)\tanh\left(\beta d/2\right)$, $\chi = 1/\left(1-\lambda^2\bar{k}_e q/\left(D\varepsilon\right)\right)$, $\omega_e = \bar{k}_e q/\varepsilon$, and $\bar{k}_e = k_{+,e}-k_{-,e}$. Equation (20) is a very general extension of the PNP model in which the surface effects described by the boundary condition given by Eq. (16) are taken into account.

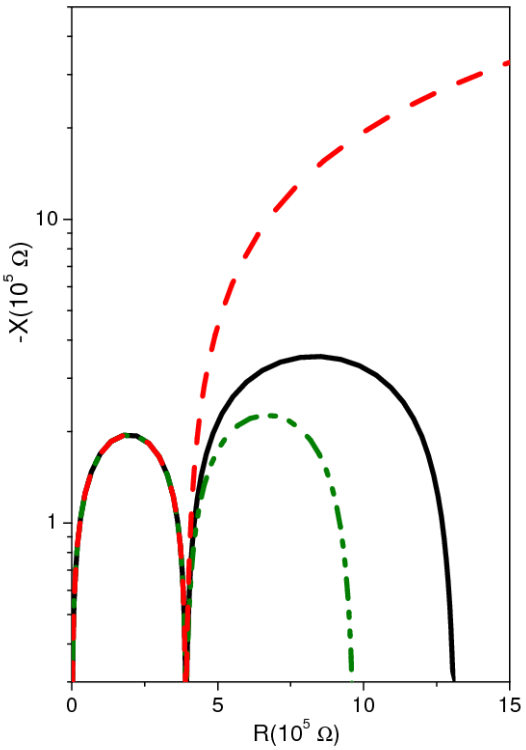

Figure 3. This figure illustrates the Nyquist diagram by considering particular situations of Eq. (20). The black (solid) line corresponds to the case $\bar{k}_e \neq 0$ with $\bar{\kappa}(i\omega) = \bar{\kappa}_2(i\omega)^{\delta_2}$, the red dashed line is the case $\bar{\kappa}(i\omega) = \bar{\kappa}_2(i\omega)^{\delta_2}$ with $\bar{k}_e = 0$, and the green dashed–dotted line is the case $\bar{\kappa}(i\omega) = \bar{\kappa}_1 + \bar{\kappa}_2(i\omega)^{\delta_2}$ with $\bar{k}_e = 0$. We considered, for simplicity, $S = \times 10^{-3}\, m^2$, $\varepsilon = 82\varepsilon_0$, $D = 2.0\times10^{-9}\, m^2/s$, $d = 10^{-3}\, m$, $\bar{\kappa}_1 = 10^{-6}\mathrm{m/s}$, $\bar{k}_e = 8\times10^9\,(Vms)^{-1}$, $\delta_2 = 0.8$, and $\bar{\kappa}_2 = 10^{-6}\mathrm{m/s}^{1-\delta_2}$, and $\lambda = 7.43\times10^{-7}\, m$.

Figure 3 illustrates the behavior of Eq. (20) in different situations. It shows that the low frequency behavior is essentially governed by the Ohmic term when $\bar{\kappa}(i\omega) \propto (i\omega)^{\delta}$. The case $\bar{\kappa}(i\omega) = constant$ represents an interplay between this effect and the one exhibited by the Ohmic term.

5. EXPERIMENTAL DATA AND MODEL

Now, we apply the previous results to describe the experimental behavior exhibited in Fig. 4 for the Milli – Q water and a weak electrolyte (KCl with $3.3\times10^{-4}\ Mol/l$). The experiement was performed by using a Solartron SI 1290 A impedance-gain phase analyzer in the frequency interval 10 mHz to 10.0 MHz, as described in Ref. [28]. In particular, the sample holder is composed by two circular stainless steel electrodes, each one with an area $S = 3.14cm^2$ opposite to each other, separated by a distance of $d = 1.0mm$. The Milli-Q water and the solution of KCl were placed between these electrodes, in a volume of $0.314mL$ and the measure of for which one was performed. To avoid any kind of unwanted substance that could, somehow, affect the EIS data, the electrodes were cleaned with a smooth sponge and neutral detergent and rinsed with Milli-Q water. After they were cleaned a few times, they were left in an ultrasonic bath of acetone ($C_3H_6O\ molar\ mass = 58.08gmol^{-1}$) for ten minutes. To put the electrodes on the sample holder, tweezers were used, to abstain the surfaces of oiliness that could come from the skin.

We observe from the experimental data that the electrical response can not be suitable described in all range of frequency if we consider the PNP model with perfect blocking boundary conditions. We need to take into account additional effects related to the surface which imply in extend Eq. (4). An extension by incorporating the Chang – Jaffé condition [37] on the surface is useful for the KCl in the very low frequency limit, i.e., $f < 10^{-1}\text{Hz}$ for the experimental data presented in Fig.3. For the Milli – Q water and also for the KCl (in the intermediate range of frequency, i.e., $10^{-1}\text{Hz} - 10^{3}\text{Hz}$) the impedace behaves as $Z \sim 1/(i\omega)^{\delta}$ which is very different from the behavior $Z \sim 1/(i\omega)$ obtained from Eq. (4). This behavior which in general is reproduced by means of constant phase elements can be obtained from Eq. (16) by a suitable choice of $\kappa(t,\eta)$ as illustrated in Fig. 3 and, consequently, enable us to describe the experimental data. In particular, $\delta \neq 1$ with $0 < \delta < 1$ is an intermediate between a capacitive ($\delta = 1$) and resistive element ($\delta = 0$) used to describe the charge accumulation on the surface of the electrodes.

6. DISCUSSION

From the analysis presented in previous section concerns the experimental data and the model, we have verified that a suitable description of the experimental data is obtained when the boundary conditions are extended by using fractional time. This extension of the differential operators to a nonintegers orders enables us to obtain a suitable behavior for the impedance which is able to describe the behavior of the experimental data. The previous results are also an evidence that the in the low frequency limit the electrical response of these electrolytical cells is essentially governed by the

surface effects, i.e., the interaction electrode – eletrolyte, and has a direct influence on the dynamic of the ions in the bulk. This point has been investigated in Ref. [46] by analyzing the behavior of the electrical conductivy and its connection with the dynamic of the ions by using the approach employed in Ref. [47,48]. In particular, the results have evidenced that the ion motion may be related to an anomalous diffusion when the behavior $Z \sim 1/(i\omega)^{\gamma}$ is manifested by the samples in the limit of low frequency, instead of the typical capacitive behavior $Z \sim 1/(i\omega)$.

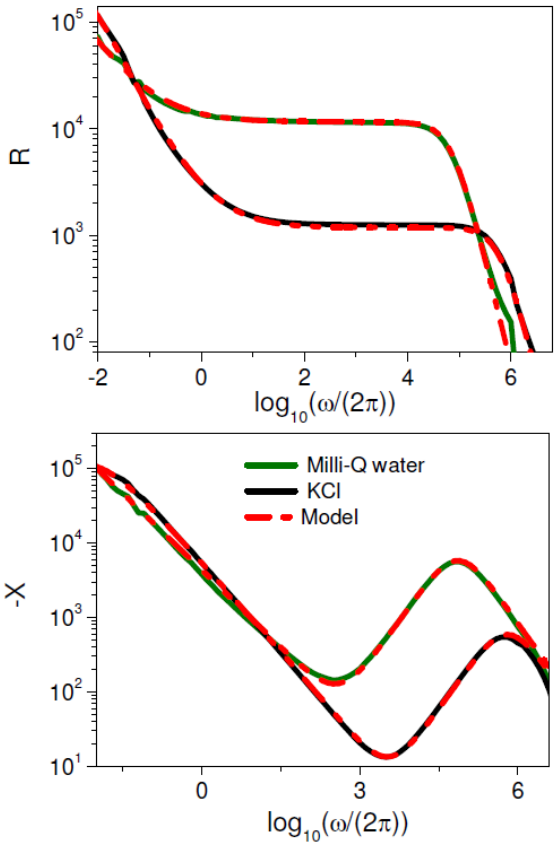

Figure 4. This figure shows the real and imaginary parts of the impedance for the Milli – Q water (green solid line) and a solution of KCl (3.3×10^{-4} *Mol/l*) (black solid line). The model is represented by the red dashed – dotted line. The best fit for the Milli – Q water was found by using Eq. (16) with $\bar{\kappa}(i\omega) = \bar{\kappa}(i\omega)^{\delta}$, $\varepsilon = 70\varepsilon_0$, $D = 3.2\times10^{-9}\ m^2 s^{-1}$, $\lambda = 3.93\times10^{-8}\ m$, and $\delta = 0.68$. For the KCl was used $\bar{\kappa}(i\omega) = \bar{\kappa}_1 + \bar{\kappa}_2(i\omega)^{\delta_2}$, $\varepsilon = 78\varepsilon_0$, $D = 6.2\times10^{-9}\ m^2 s^{-1}$, $\bar{\kappa}_1 = 10^{-6} ms^{-1}$, $\delta_2 = 0.78$, and $\bar{\kappa}_2 = 10^{-6} ms^{-1+\delta_2}$, and $\lambda = 3.98\times10^{-8}\ m$. The values of the others parameters are $S = 3.14\times10^{-3}\ m^2$, $d = 10^{-3}\ m$.

Similar features are expected for the experimental scenarios described above for the electrolytic cell with Milli – Q water or a weak eletrolyte of KCl leading us to an anomalous diffusion. In fact, in this limit the behavior of the electrcial conductivity is usually $\sigma \approx \sigma_0 + \sigma_\delta \omega^{\delta}$ which implies in different regimes of diffusion. This behavior for the electrical conductivity with an unusual frequency dependence can be directly connected to the behavior of the impedance $Z \sim 1/(i\omega)^{\delta}$ which

is not present in the standard approches for $\omega \to 0$. Thus, a suitable description of the behavior manifested by the experimental data needs to take into account these features which are not present in the standard approach when the low frequency limit is considered. In the context of equivalent circuits the presence of this unusual leads us to use constant phase elements to reproduce the behavior of the experimental data. It is worth mentioning that the constant phase elements can be related to the Eq.(16) as shown in Ref. [32,49] by a suitable choice of $\kappa(t,\bar{\eta})$. Another approach which may be used to investigate the electrical response is based on the Debye − Falkenhagen equation for the potential by considering that the total impedance is a sum of two contributions [50,51] one of them comes from the compact layer impedance and the other from the diffusive layer. It is worth mentioning that to describe the compact layer the behavior of a constant phase element [52] behavior is incorporated in this part of the impedance.

7. CONCLUSION

We have reviewed for the PNP – model some extensions based on the fractional calculus. The first extension has considered the presence of fractional time derivative of distributed order in the bulk equation. This extension has shown a direct effect on the real part of the impedance in the low frequency regime (see Fig. 1a). For the imaginary part of the impedance, the influence of the fractional derivative of distributed order may be verified in the intermediary frequency range (see the green and red lines of Fig. 1b). The imaginary part of the impedance in the low frequency limit is not influenced by this extension, as shown in Fig. 1b. Surface effects as, for instance, adsorption – desorption phenomena and charge transfer which are pronounced in the low frequency regime and frequently characterized by $Z:\ 1/(i\omega)^{\delta}$ $(0<\delta\leq 1)$, may not be suitably described by the conventional models and require different boundary conditions to be accounted for. As a matter of fact, in many situations the behavior of the impedance in this limit is given by $Z:\ 1/(i\omega)^{\delta}$ with $\delta \neq 1$. For this important experimental reason, we have incorporated fractional time derivatives to the boundary condition to describe, from the phenomenological point of view, the behavior of the experimental data (see, for instance, Refs. [29]). The boundary conditions, Eq. (16), analyzed in Sec. 4, have many particular cases, but the Ohmic case requires an additional term. This has been also discussed in Sec. 4 by considering Eq. (19) which yielded Eq. (20) for the impedance. We have applied these results to describe the experimental data presented in Sec. 5. In particular, we have obtained a good agreement between the experimental data and the model and a discussion about the experimental results and the model is presented in Sec. 6. The extension of the PNP – model to the context of the fractional calculus discussed here may be useful to understand the electrical response when the standard approach is not successful enough to face the high complexity of the experimental data.

ACKNOWLEDGEMENT
This work has been partially supported by the National Institute of Science and Technology for Complex Systems (INCT - SC, Rio de Janeiro, Brazil) and the National Institute of Science and Technology of Complex Fluids (INCT-Fcx, São Paulo, Brazil). EKL also thanks the financial support of the CNPq under the Grant No. 303642/2014-9.

References

1. C. Tadjeran, M. M. Meerschaert and S. Hans-Peter, *J. Comp. Phys.*, 213 (2006) 205.
2. P. Zhuang, F. Liu, V. Anh and I. Turner, *SIAM J. Numer. Anal.*, 47 (2009) 1760.
3. Q. Yang, I. Turner, F. Liu and M. Ilic, *SIAM J. Sci. Comput.*, 33 (2011) 1159.
4. E. J. S. Pires, J. A. T. Machado and P. B. M. Oliveira, *Signal Process.*, 83 (2003) 2377.
5. A. Carpinteri, B. Chiaia and P. Cornetti, *Comput. Method Appl. Mech.*, 191 (2001) 3.
6. K. R. Sreenivasan, *Fractals*, 2 (1994) 253.
7. N. Laskin, *Phys. Rev. E*, 62 (2000) 3135.
8. H. Kleinert, *EPL (Europhysics Letters)*, 100 (2012) 10001.
9. D. A. Robinson, *Ann. Rev. Neurosci.*, 4 (1981) 462.
10. E. Barsoukov and J. R. Macdonald, Impedance Spectroscopy: Theory, Experiment, and Applications, Wiley, (1987) New York, USA.
11. G. Barbero and L. R. Evangelista, Adsorption Phenomena and Anchoring Energy in Nematic Liquid Crystals, Taylor & Francis, (2006) London, UK.
12. J. E. B. Randles, *Disc. Far. Soc.*, 1 (1947) 11.
13. B. B. V. Ershler, *Disc. Far. Soc.*, 1 (1947) 269.
14. F. Batalioto, A. R. Duarte, G. Barbero and A. M. N. Figueredo, *J. Phys. Chem. B*, 114 (2010) 3467.
15. I. S. Jesus and J. A. T. Machado, *Nonlinear Dynam.*, 56 (2009) 45.
16. I. S. Jesus and J. A. T. Machado, *Math. Prob. Eng.*, 2012 (2012) 248175.
17. J. Bisquert, *Phys. Rev. Lett.*, 91 (2003) 010602.
18. P. A. Santoro, J. L. de Paula, E. K. Lenzi and L. R. Evangelista, *J. Chem. Phys.*, 135 (2011) 114704.
19. J. Bisquert and A. Compte, *J. Electroanal. Chem.*, 499 (2001) 112.
20. J. Bisquert, G. Garcia-Belmonte and A. Pitarch, *ChemPhysChem*, 17 (2003) 287.
21. J. Bisquert, *Phys. Rev. E*, 72 (2005) 011109.
22. E. Warburg, *Drud. Ann. der Phys.*, 6 (1901) 125.
23. G. Barbero, *Phys. Chem. Chem. Phys.*, 18 (2016) 29537.
24. J. L. de Paula, P. A. Santoro, R. S. Zola, E. K. Lenzi, L. R. Evangelista, F. Ciuchi, A. Mazzulla and N. Scaramuzza, *Phys. Rev. E*, 86 (2012) 051705.
25. E. K. Lenzi, L. R. Evangelista and G. Barbero, *J. Phys. Chem. Lett.* B, 113 (2009) 11371.
26. P. A. Santoro, E. K. Lenzi, L. R. Evangelista, F. Ciuchi, A. Mazzulla and N. Scaramuzza, *Mol. Cryst. Liq. Crist.*, 576 (2013) 23.
27. F. Ciuchi, A. Mazzulla, N. Scaramuzza, E. K. Lenzi and L. R. Evangelista, *J. Phys. Chem. C*, 116 (2012) 8773.
28. E. K. Lenzi, P. R. G. Fernandes, T. Pretucci, H. Mukai, H. V. Ribeiro, M. K. Lenzi and G. Gonçalves, *Int. J. Electrochem. Sci.*, 8 (2013) 2849.
29. E. K. Lenzi, R. S. Zola, R. Rossato, H. V. Ribeiro, D. S. Vieira and L. R. Evangelista, *Electrochim. Acta*, 226 (2017) 40.
30. E. K. Lenzi, P. R. G. Fernandes, T. Petrucci, H. Mukai and H. V. Ribeiro, *Phys. Rev. E*, 84 (2011) 041128.
31. E. K. Lenzi, M. K. Lenzi, F. R. G. B. Silva, G. Gonçalves, R. Rossato, R. S. Zola and L. R. Evangelista, *J. Electroanal. Chem.*, 712 (2014) 82.
32. F. R. G. B. Silva, H. V. Ribeiro, M. K. Lenzi, T. Petrucci, F. S. Michels and E. K. Lenzi, *Int. J. Electrochem. Sci.*, 9 (2014) 1892.
33. T. Basu, M. M. Goswami, T. R. Middya and S. Tarafdar, *J. Phys. Chem., B* 116 (2012) 11362.
34. J. B. Bates, Y. T. Chu and W. T. Stribling, *Phys. Rev. Lett.*, 60 (1988) 627.
35. G. Barbero, F. Batalioto and A. M. N. Figueiredo, *Appl. Phys. Lett.*, 92 (2008) 172908.
36. A. L. Alexe-Ionescu, G. Barbero and I. Lelidis, *J. Phys. Chem. B*, 113 (2009) 14747.

37. H. Chang and G. Jaffé, *J. Chem. Phys.*, 20 (1952) 1071.
38. I. Lelidis, J. R. Macdonald and G. Barbero, *J. Phys. D*, 49 (2016) 025503.
39. I. Podlubny, Fractional Differential Equations, Academic Press, (1999) San Diego, USA.
40. E. K. Lenzi, R. S. Mendes and C. Tsallis, *Phys. Rev. E*, 67 (2003) 031104.
41. A. A. Tateishi, E. K. Lenzi, L. R. da Silva, H. V. Ribeiro, S. Picoli Jr. and R. S. Mendes, *Phys. Rev. E*, 85 (2012) 011147.
42. L. R. Evangelista, E. K. Lenzi, G. Barbero and J. R. Macdonald, *J. Phys. Condens. Matter*, 23 (2011) 485005.
43. E. K. Lenzi, L. R. Evangelista, G. Barbero and F. Mantegazza, *EPL (Europhysics Letters)*, 85 (2004) 28004.
44. E. K. Lenzi, C. A. R. Yednak and L. R. Evangelista, *Phys. Rev. E*, 81 (2010) 011116.
45. V. G. Guimaraes, H. V. Ribeiro, Q. Li, L. R. Evangelista, E. K. Lenzi and R. S. Zola, *Soft Matter*, 11 (2015) 1658.
46. E. K. Lenzi, R. S. Zola, H. V. Ribeiro, Denner S. Vieira, F. Ciuchi, A. Mazzulla, N. Scaramuzza and L. R. Evangelista, *J. Phys. Chem. B*, 121 (2017) 2882.
47. H. Scher and M. Lax, *Phys. Rev. B*, 7 (1973) 4491.
48. H. Scher and M. Lax, *Phys. Rev. B*, 7 (1973) 4502.
49. E. K. Lenzi, J. L. de Paula, F. R. G. B. Silva and L. R. Evangelista, *J. Phys. Chem. C*, 117 (2013) 23685.
50. M. B. Singh and R. Kant, *J. Phys. Chem. C*, 118 (2014) 5122.
51. M. B. Singh and R. Kant, *J. Electroanal. Chem.*, 704 (2013) 197.
52. T. Pajkossy, *Solid State Ionics*, 76 (2005) 1997.